

Accepted Manuscript

Formation of a bile salt-drug hydrogel to predict human intestinal absorption

Dina S. Shokry, Laura J. Waters, Gareth M.B. Parkes, John C. Mitchell, Martin J. Snowden



PII: S0022-3549(18)30602-6

DOI: [10.1016/j.xphs.2018.10.005](https://doi.org/10.1016/j.xphs.2018.10.005)

Reference: XPHS 1312

To appear in: *Journal of Pharmaceutical Sciences*

Received Date: 23 July 2018

Revised Date: 2 October 2018

Accepted Date: 3 October 2018

Please cite this article as: Shokry DS, Waters LJ, Parkes GMB, Mitchell JC, Snowden MJ, Formation of a bile salt-drug hydrogel to predict human intestinal absorption, *Journal of Pharmaceutical Sciences* (2018), doi: <https://doi.org/10.1016/j.xphs.2018.10.005>.

This is a PDF file of an unedited manuscript that has been accepted for publication. As a service to our customers we are providing this early version of the manuscript. The manuscript will undergo copyediting, typesetting, and review of the resulting proof before it is published in its final form. Please note that during the production process errors may be discovered which could affect the content, and all legal disclaimers that apply to the journal pertain.

1 Formation of a bile salt-drug hydrogel to predict human intestinal absorption

2

3 Dina S. Shokry^b, Laura J. Waters^{*a}, Gareth M. B. Parkes^a, John C. Mitchell^b, and Martin J
4 Snowden^b

5 ^a School of Applied Sciences, University of Huddersfield, Queensgate, Huddersfield, HD1
6 3DH, UK,

7 ^b Faculty of Engineering and Science, Medway Centre for Formulation Science, University of
8 Greenwich, Chatham, Kent ME4 4TB, UK.

9

10 *Corresponding author: l.waters@hud.ac.uk

11

12 ABSTRACT

13

14 The unique character of bile salts to self-assemble into hydrogels in the presence of halide
15 salts was exploited in this work to facilitate the prediction of human intestinal absorption
16 (%HIA) for a set of 25 compounds. This was achieved by firstly incorporating each
17 compound separately within the process of gel formation to create a series of gel-drug
18 membranes. Scanning Electron Microscopy (SEM) analysis of the freeze-dried samples of the
19 blank bile salt hydrogels and drug loaded bile salt hydrogels indicated a unique
20 microstructure made of a network of intertwined fibrils. Drug-loaded sodium deoxycholate
21 (NaDC) hydrogels were then utilised as the donor phase to study permeability using flow-
22 through and static diffusion cells. The resulting values of the release-permeability coefficient
23 (K_p) were then analysed, along with other molecular descriptors, for the prediction of human
24 intestinal absorption (%HIA) using multiple linear regression (MLR). Overall, when
25 comparing predicted values (using the systems presented in this study) with known literature
26 values, it can be seen that both methods (i.e. using static and flow through cells) had good
27 predictability with R^2_{PRED} values of 79.8 % and 79.7 % respectively. This study therefore
28 proposes a novel, accurate and precise way to predict human intestinal absorption for
29 compounds of pharmaceutical interest using a simple *in vitro* permeation system. It is
30 important to develop alternatives to the current methods used in prediction of HIA which are
31 expensive and time consuming or include the use of animals. Therefore, the proposed method
32 in this study being economic and time saving provides superiority over these current methods
33 and suggests the possibility of its use as an alternate to such methods for prediction of HIA.

34 **Statistical Summary:** 7648 words, 3 tables, 9 figures, 24 pages

35

36 **Declaration of Interest: None.**

37 **Keywords:** sodium deoxycholate; NaDC; human intestinal absorption; %HIA; hydrogels;
38 flow-through cells; static diffusion cells; absorption; permeation

39

40 **1. Introduction**

41 Due to convenience of the oral route of administration, most of the pharmaceutical
42 compounds are formulated as orally administered drugs. However, the properties of some
43 compounds can be incompatible with oral administration. In fact, the pharmaceutical industry
44 suffers from major financial losses because of the poor bioavailability of some new drugs
45 after their oral administration, only discovered once in the clinical development stage¹⁻
46 ⁴.Therefore, poor drug candidates with poor biopharmaceutical properties, such as poor oral
47 bioavailability, and aqueous solubility should be identified as soon as possible before
48 entering the clinical development stage in which the cost of research performed for a
49 compound is significantly high. As a result, there has been a growing interest in the early
50 prediction of biopharmaceutical properties by means of experimental and theoretical models.
51 This study provides a rapid and cheap method for the prediction of one of the most important
52 pharmacokinetic properties of pharmaceutical compounds which is intestinal absorption
53 through the use of bile salts. The number of recent publications on the physiological
54 importance of bile salts reflects a growing interest in this area. It has been found that certain
55 bile salts, such as sodium deoxycholate (NaDC), are capable of self-assembling into gels
56 through a process driven by the balance of hydrophobic interactions, hydrogen-bonding, van
57 der Waals forces and steric effects⁵⁻⁹. The hydrogels made from bile salts are very different
58 from polymeric gels (which are made from chemical cross-linking) and have specific and
59 vital roles within the body. Bile salts are a group of cholic acid derivatives, known as
60 biosurfactants, that have an amphiphilic structure with a steroidal backbone; a distinctive
61 structure that differentiates this class of surfactants from conventional synthetic surfactants⁹;
62 ¹⁰. Some important biological functions, such as cholesterol solubilisation, dietary fat and fat
63 soluble vitamin absorption as well as removal of fatty acids from pancreatic hydrolysis, are
64 carried out by the aggregates resulting from the self-assembly of bile salts occurring as a
65 result of their unusual structure^{9, 11-13}.

66 Biocompatible fragment containing hydrogels, such as amino acid derivatives¹⁴, peptides^{15, 16},
67 cholic acid¹⁷ derivatives and carbohydrate systems^{18, 19}, have been given notable attention
68 because of one key benefit, namely their safe use in biomedical applications. The presence of
69 halide salts has been shown to improve the production of bile salt formed hydrogels^{20, 21}. The
70 formation of these hydrogels is through a network of intertwined fibrils formed by massive
71 cycles of bile salt molecules attached together by noncovalent interactions, especially
72 hydrogen-bonds. It was found that NaCl had a prominent effect on encouraging the gelation
73 of NaDC solutions to form supramolecular hydrogels with higher gelation capability and
74 mechanical force because of the small radius of hydration of the NaCl ions²⁰. An important
75 role is played by both sodium and the chloride ions in the formation of the hydrogels by
76 reducing the electrostatic repulsion between NaDC polar heads therefore contributing to the
77 compression of the thickness of the electric double layer²⁰. Furthermore, weak coordination
78 bonds form between sodium ions and carboxylate groups, stimulating connection of the polar
79 head of carboxyl groups via hydrogen-bonding which leads to the formation of a more
80 regular crystalline interface thus shifting the growth of aggregates along one direction
81 towards fibrous aggregate formation^{22, 23}. In addition, the chloride ions play a role in hydrogel
82 formation, as well as the weak electrostatic interaction which is thought to exist between the
83 sodium salt anion (chloride ions) and the α -methylene attached to the carboxylate group of
84 the bile salt²⁴. NaDC solutions have been reported in literature to give highly viscous gels by
85 the formation of polymer-like aggregates at pH values less than 7.8 (Figure 1)^{25, 26}. However,
86 such systems have never been formulated in the presence of pharmaceutical compounds, such
87 as those considered in this work.

88

89

90 Determining human intestinal absorption is a complex, expensive and lengthy process yet is
91 necessary to understand the behaviour of pharmaceutical compounds *in vivo*. Developed
92 systems to predict absorption are highly sought-after and seek to provide a simpler, less
93 expensive and more ethically acceptable method to predict intestinal absorption. Several
94 techniques have previously been employed to predict intestinal absorption including cell
95 culture based models²⁷, such as Caco-2 cells²⁸⁻³⁵, membrane based models, such as
96 PAMPA³⁶⁻³⁹, *ex-vivo* models, such as Ussing chambers⁴⁰⁻⁴², *in situ* intestinal perfusion
97 models⁴³⁻⁴⁶ and everted intestinal ring/sac⁴⁷. Models using spectroscopic⁴⁸ and
98 chromatographic⁴⁹ properties have previously been developed by the authors of this study.
99 This work however, presents the creation of a novel drug-gel bile salt based product as the

100 basis of the analytical donor phase to determine permeation which can ultimately lead to
101 prediction of intestinal absorption. The synthesised hydrogel was used as a donor phase in
102 both static diffusion and flow-through cells, with a permeable dialysis membrane for support,
103 to determine the release-permeability coefficient (K_p) of the studied drugs. This was then
104 statistically analysed for developing models for prediction of human intestinal absorption.

105

106 **2. Experimental**

107 **2.1 Chemicals and materials**

108 Sodium deoxycholate (NaDC, 97 %), sodium chloride (NaCl, analytical grade), sodium
109 dihydrogen orthophosphate dihydrate ($\text{NaH}_2\text{PO}_4 \cdot 2\text{H}_2\text{O}$, 99 %), disodium hydrogen
110 orthophosphate anhydrous (Na_2HPO_4 , 99 %) were purchased from Fisher Scientific,
111 Loughborough, UK. The compounds of pharmaceutical interest considered in this work were:
112 caffeine 97 % (Sigma Aldrich, Dorset, UK), fenopfen 97 % (Fluka, Dorset, UK), quinine
113 96 % (Fluka, Dorset, UK), acetaminophen 99 % (Sigma Aldrich, Dorset, UK), leflunomide
114 98 % (Sigma Aldrich, Dorset, UK), linezolid >98 % (Sigma Aldrich, Dorset, UK), ketoprofen
115 98 % (Sigma Aldrich, Dorset, UK), lidocaine 98 % (Sigma Aldrich, Dorset, UK),
116 indomethacin 99 % (Sigma Aldrich, Dorset, UK), phenylbutazone 99 % (Sigma Aldrich,
117 Dorset, UK), fluconazole 98 % (Sigma Aldrich, Dorset, UK), carbamazepine 99 % (Sigma
118 Aldrich, Dorset, UK), cimetidine (Sigma Aldrich, Dorset, UK), moexipril >98 % (Sigma
119 Aldrich, Dorset, UK), naproxen 98 % (Sigma Aldrich, Dorset, UK), piroxicam 98 % (Sigma
120 Aldrich, Dorset, UK), zolmitriptan >98 % (Sigma Aldrich, Dorset, UK), haloperidol 99 %
121 (Sigma Aldrich, Dorset, UK), fosinopril >98 % (Sigma Aldrich, Dorset, UK), ibuprofen 98 %
122 (BASF, Cheshire, UK), diclofenac 98 % (TCI Europe, Zwijndrecht, Belgium), flurbiprofen
123 98 % (TCI Europe), gemfibrozil 98 % (TCI Europe), theophylline 98 %, (TCI, Oxford, UK)
124 and meloxicam 98 % (TCI Europe). Dialysis membrane was a high retention, seamless,
125 cellulose tubing with an average flat width of 23 mm and molecular weight cut off (MWCO)
126 of 12400.

127 **2.2 Saturated solubility analysis**

128 Wavelength of maximum absorption (λ_{max}) of each compound was determined by scanning
129 its solution within (200-400 nm) using UV spectrophotometer. An excess amount of each of
130 the drugs was added to 5 mL of phosphate buffer (0.2 M disodium orthophosphate, sodium
131 dihydrogen orthophosphate and sodium chloride at a pH of 7.4) in 7 mL vials, then sealed
132 and stored at 37 °C. The solutions were then filtered through 0.45 μm Nylon filters to

133 remove excess solid, diluted by known amounts using buffer, then assayed using UV
134 spectrophotometry at the pre-determined λ_{\max} and compared with an already established
135 calibration plot. A calibration plot was established for each compound by preparing a
136 standard stock solution of each compound, in the previously mentioned buffer/salt mixture at
137 pH 7.4, from which different volumes were aliquoted out and diluted accordingly for
138 preparation of different dilutions of the compound. The dilutions were then scanned for
139 measuring the absorbance and a plot of the compound concentrations against its
140 corresponding absorbances was then constructed.

141 **2.3 Preparation of bile salt hydrogel with infinite dose of drug**

142 An NaDC-based hydrogel (70 mM) was prepared by gradually adding a specified volume of
143 phosphate buffer (composition described above). Based on the saturation solubility results,
144 the infinite dose for each of the drugs under study was calculated where an accurately
145 weighed amount of each of the drugs under study was added to an accurately weighed
146 amount of NaDC (580.4 mg) in a 50 mL beaker for the formation of a 20 mL drug saturated
147 hydrogel. The mixture of NaDC and drug in buffer was then sonicated in an ultrasonic water
148 bath for 2 minutes at room temperature until the consistency of the solution thickened and the
149 gel began to form so the gelation process was visually judged. The gel was left stirring after
150 sonication and then allowed to stand for 24 hours to ensure homogenous distribution of the
151 drug throughout the gel.

152 **2.4 Analytical Instrumentation**

153 **2.4.1 Diffusion cells**

154 Diffusion cells have been classically considered to be one of the more popular methods used
155 in prediction of permeation of drugs and chemicals across the skin^{50, 51}. Both static (Franz-
156 type) cells and continuous flow (flow-through) cells were used in this study whereby the
157 setup of both types of diffusion cells have donor and receptor compartments with a
158 membrane mounted between and a water jacket to achieve a consistent temperature of 37 °C.
159 Sink conditions were maintained in both types of cells.

160 **2.4.1.1 Static diffusion cells**

161 A set up of six 30 mL vertical Franz cells, bespoke, were used in the study of the permeation
162 of drugs from the drug-saturated hydrogels in the donor chamber to buffer in the receptor
163 chamber per experiment. Each cell was formed of two chambers; donor and receptor
164 chambers held together by clamps with a dialysis membrane fitted to cover the diffusion area

165 (3.14 cm²) mounted between the two chambers as a support for the hydrogel. A 5 mL sample
166 of the drug-saturated hydrogel was placed in the donor chamber while the clean, dried
167 receptor chamber was filled with deaerated buffer and allowed to equilibrate at 37 °C. All
168 openings, including donor top and receptor arm, were occluded to prevent evaporation. The
169 receptor compartment was stirred at 450 rpm using a magnetic stirrer. Samples (1 mL) were
170 extracted at 45 minute intervals over a 6 hour period and analysed using UV
171 spectrophotometry at the λ_{\max} of each drug. After each extraction, 1mL of fresh, deaerated
172 buffer was introduced into the receptor.

173 **2.4.1.2. Flow-through diffusion cells**

174 A set up of six flow through cells were used per experiment (purchased from PermeGear Inc.,
175 Hellertown, PA 18055 USA). Each cell consisted of two compartments; the donor and the
176 receptor compartments fixed together by clamps and screws with a dialysis membrane cut
177 down to cover the diffusion area (0.554 cm²) as a support for the hydrogel. 0.8 mL of the
178 drug saturated hydrogel was placed in the donor chamber while buffer was pumped
179 continuously through the six receptor compartments at a flow rate of 0.52 mL/min using a
180 peristaltic pump. All the cells were kept at a temperature of 37 °C using a heat conducting
181 cell holder. The donor compartments were covered with moisture-resistant film (Parafilm M,
182 Alcan packaging) to avoid drying of the hydrogel. Samples from the six cells were collected
183 in 7 mL vials every 45 minutes over a 6-hour period and analysed using UV
184 spectrophotometry at the λ_{\max} of each drug.

185 All spectrophotometric analysis was undertaken using an Agilent Model Cary 60 UV-Vis
186 fitted with a Cary single cell Peltier accessory to keep the samples in the sample compartment
187 at the specified temperature. A quartz cuvette of 10 mm internal thickness was used in all
188 measurements.

189

190 **2.4.2 Scanning Electron Microscopy (SEM)**

191 Electron micrographs of hydrogel with no drug as well as hydrogels saturated with each of
192 the following drugs (carbamazepine and meloxicam) were obtained using a scanning electron
193 microscope (Leica Cambridge S360, UK) operating at 15 kV. The hydrogel samples were
194 freeze dried using (CHRIST ALPHA 2 - 4 LD plus) and mounted on a metal stub with
195 double-sided adhesive tape and coated under vacuum with gold in an argon atmosphere prior
196 to observation. Micrographs with different magnifications were taken to facilitate the study of
197 the morphology of the hydrogels.

198 2.4.3 Fourier transform infrared (FT-IR)

199 The FT-IR spectra (650-4000 cm^{-1}) of hydrogels saturated with (caffeine, carbamazepine,
200 fluconazole, meloxicam and piroxicam) each of the previously mentioned drugs under study
201 were air dried then recorded using ATR with a FT-IR spectrophotometer (PerkinElmer, UK).
202 Spectra with sharp peaks of reasonable intensity were obtained to consider the stability of the
203 hydrogel after the addition of the drugs.

205 2.5 Calculations:

206 2.5.1 Calculation of permeability coefficient (K_p):

207 Since the drug was added to the hydrogel in an infinite dose, the permeability coefficient (K_p)
208 can be calculated from the following relationship⁵² :

$$209 K_p = Q / [A \cdot t \cdot (C_o - C_i)]$$

210
211 Where:

212 Q : the quantity of drug transported through the hydrogel in time t (min).

213 C_o : the concentration of the drug in the donor chamber (saturated solubility concentration in
214 the buffer used).

215 C_i : is the concentration of the drug in the receptor chamber.

216 A : the area of the exposed hydrogel in cm^2 .

217 Since the drug was applied to the hydrogel in an infinite dose, C_i can be simplified to zero.

218 K_p , defined as the permeant penetration rate per unit concentration, is given in cm/min and
219 assumed to be a first order process.

220 2.5.2 Statistical analysis:

221 Data analysis was conducted using Minitab 17. Multiple linear regression analysis was
222 conducted where all the molecular descriptors were included and regressed against the
223 dependant variable %HIA and backward elimination modelling strategy. Variables with high
224 variance inflation factors (VIF) were removed to take (VIF) to acceptable limits. At the end
225 an optimum model was obtained that provided a good summary of data. The variables
226 remaining in the optimal model were assessed for significance and relative importance by
227 standardised coefficients and the associated p-values.

228 The predictive ability of the preferred model was assessed using adjusted- R^2 and R^2 for
229 prediction (R^2_{PRED}) which can indicate the predictive ability of the model itself and
230 consequently reflects the far wider ability to apply the model.

231 3. Results and discussion

232 3.1 Hydrogel formation and characterisation

233 The microstructure of the hydrogels formed by NaDC at pH 7.4 was investigated for 'blank'
234 NaDC hydrogel, as well as drug-loaded NaDC hydrogel, using scanning electron microscopy
235 (SEM). The obtained SEM observations for the blank NaDC hydrogel freeze dried samples
236 showed a network structure of intertwined fibrils with medium size pockets between (Figure
237 3).

238
239 Furthermore, the microstructure of the freeze dried samples of two selected drug loaded
240 hydrogels (carbamazepine and meloxicam) showed the same network structure as the freeze
241 dried sample of 'blank' NaDC hydrogel (Figure 4).

242
243
244 The difference in the structure of carbamazepine and meloxicam hydrogels could be
245 attributed to carbamazepine being more hydrophobic than meloxicam where the log D of
246 carbamazepine at pH 7.4 is 2.28⁵³ while that of meloxicam at the same pH is 1.04. As a
247 result, carbamazepine may have become more involved in the construction of the hydrogel
248 network thus partially interrupting the crystalline-like arrangement of NaDC molecules
249 together in the gel.

250 In contrast, the anionic drug meloxicam is less hydrophobic (log D at pH 7.4=1.04)⁵³ and has
251 a comparatively high molecular weight of 351.40 g/mol⁵³ so is less involved in the main
252 structure of hydrogel formation. Therefore, in this product the network was more compact
253 with the presence of the drug entrapped inside the network structure. This was later
254 confirmed by the higher K_p value obtained for carbamazepine than that obtained for
255 meloxicam.

256 FT-IR spectra were obtained upon drying of the sample to confirm the stability of the
257 hydrogel with the addition of the drugs. These were compared with spectra obtained from the
258 blank hydrogel samples to identify changes in the characteristic peaks (spectra presented in
259 Supplementary Information).

260 It was observed that upon the inclusion of drugs to the NaDC hydrogel there was a decrease
261 in the wave number of the O-H broad peak appearing at 3334 cm⁻¹ for the blank NaDC
262 hydrogel sample. This decrease shows destruction of H-bonding between the NaDC
263 molecules and the formation of new H-bonding between the NaDC and each drug molecule
264²⁰. The decrease was the highest in the case of carbamazepine (3233 cm⁻¹) indicating
265 carbamazepine was more involved in the hydrogel structure confirming the previous SEM

266 results for this drug. In contrast, the decrease was the least in the case of meloxicam (3327
267 cm^{-1}) showing less inclusion of this drug in the NaDC hydrogel structure thus confirming the
268 previous SEM results for meloxicam (Figure 4). No appearance of new peaks or
269 disappearance of existing peaks was observed suggesting no chemical interaction between the
270 added drugs and NaDC gel.

271 **3.2 Bile salt concentration effects**

272 In this work, a 70 mM NaDC concentration was picked for the preparation of all the drug
273 loaded hydrogels used in all the permeation studies carried out for the prediction of human
274 intestinal absorption (HIA). The selection of such value was attributed to the rate of drug
275 permeation being the highest at this concentration. Such finding was based on testing the
276 effect of the change in the hydrogel concentration from 50 to 100 mM on the release of
277 different compounds (neutral, anionic and cationic), as shown in Figure 5.

278

279 According to Figure 5, it can be observed that the permeation rate of anionic drugs
280 (flurbiprofen, gemfibrozil, ibuprofen and piroxicam) is less affected by the change in the
281 concentration of NaDC hydrogel than neutral (acetaminophen, carbamazepine and
282 fluconazole) and cationic (lidocaine) drugs. However, all the selected drugs showed the
283 highest permeation rate at 70 mM concentration of NaDC.

284 **3.3 Determination of release-permeability**

285 Based on the previous findings, an NaDC concentration of 70 mM was selected to be used in
286 a permeation study of 25 compounds where the permeation experiment for each compound
287 was carried out in triplicate. Calculated K_p values were then used in the statistical modelling
288 of human intestinal absorption. The permeability coefficient (K_p) for twenty-five compounds
289 was calculated from the slopes of the plots of cumulative amount of drug permeated through
290 the hydrogel ($\mu\text{g}/\text{cm}^2$) against time (min) obtained using both the flow through and static cell
291 techniques as shown in Figures 6 and 7. The dialysis membrane works only as a support for
292 the hydrogel to prevent it from falling into the receiver chamber. Since the MWCO of the
293 used dialysis support is 12400, it will retain compounds of a molecular weight of 12400 or
294 greater so the studied compounds in solution or in hydrogel are expected to move freely with
295 the buffer movement from the donor to the receiver chamber without being retained.
296 Although the hydrogels were prepared in a manner such that the compounds under study
297 saturated it, these compounds are completely soluble in the hydrogel matrix therefore
298 allowing the drug molecules to move with the buffer from the gel donor chamber to the
299 receiver chamber without any hindrance from the dialysis support. For comparison, the

300 permeability coefficient was determined for eight selected drugs using only buffer pH 7.4
301 with no NaDC hydrogel and it was found to be always higher in buffer than in hydrogel
302 except for acetaminophen which could be attributed to that acetaminophen was the only drug
303 with significant aqueous solubility, a low molecular weight (151.2 g/mol)⁵³ and was the least
304 lipophilic ($\log P_{o/w} = 0.46$) of all the studied drugs⁵⁴.

305 Although the sample volume in the donor chamber when using static cells (5 mL) was higher
306 than when using flow through cells (0.8 mL), less permeation of the studied compounds was
307 observed with the static cells than the flow through cells. This could be attributed to the
308 bigger receptor chamber volume of the static cells used (30 mL) than the flow through cells
309 (1.5 mL of the receptor phase was collected every 45 min).

310

311 **3.4 Statistical modelling of human intestinal absorption (HIA)**

312 For the prediction of human intestinal absorption (HIA), the obtained permeability
313 coefficients (K_p) from both flow through and static cells were statistically analysed alongside
314 the reported values of some molecular descriptors such as molecular weight (Mwt), polar
315 surface area (PSA), freely rotating bonds (FRB), molar volume (V_M), dissociation constant
316 (pK_a), aqueous solubility (S_w), number of hydrogen bond donors (nHD) and number of
317 hydrogen bond acceptors (nHA) against literature values of human intestinal absorption
318 (HIA) using multiple linear regression. Twenty-five drugs were selected to be used in the
319 statistical modelling of human intestinal absorption. These drugs are of a wide variety of
320 physicochemical properties (Mwt, PSA, S_w , RB, nHD, nHA and V_M) and having a wide
321 range of %HIA reported values within (23-100 %) (Tables 1-3).

322 A linear relationship was found between reported (%HIA) and experimental K_p values but
323 $\text{logit}(\text{HIA})$ was used to improve this relationship as seen in studies of a similar type⁵⁵⁻⁵⁷. The
324 human intestinal absorption values were transformed to logit by substitution in the following
325 equation, where %HIA = %Human Intestinal Absorption.

$$326 \quad \text{logit}(\% \text{HIA}) = \log (\% \text{HIA} / (100 - \% \text{HIA}))$$

327 Therefore, all drugs with % HIA values of 100 or 0 % from the training set were removed for
328 simplification.

329 Eighteen drugs were used in the development of the final models. K_p , alongside the molecular
330 descriptors (nHD and V_M) were included in the final models of both techniques.

331

332

333

334 Modelling of Human intestinal absorption using flow-through cells:

335 The following model was obtained for the prediction of HIA using flow-through cells:

336
$$\text{logit HIA} = -0.59 - 0.5522 \text{ nHD} - 0.006085 V_M - 0.765 \log K_p$$

337 The model's $R^2 = 87.58\%$, $R^2_{\text{adjust.}} = 84.92\%$, $R^2_{\text{PRED}} = 79.80\%$, $S = 0.267$

338 A 95 % confidence interval for $\log K_p$ is given by (-1.19, -0.34). t-statistic and standardised
339 coefficient of $\log K_p$ are -3.86 ($p < 0.05$) and -0.397 respectively suggesting the statistical
340 significance of $\log K_p$ as a predictor. Also the F-ratio of the overall model is statistically
341 significant, $F = 32.90$ and P value 0.000 ($p < 0.05$). Absence of autocorrelation in the current
342 regression model was proved by a Durbin- Watson statistic value of 2.532. There was no
343 marked relationship between residuals and predicted values. Seven compounds
344 (carbamazepine, fenoprofen, linezolid, naproxen, piroxicam, quinine and zolmitriptan) were
345 used for testing the obtained model as shown in Table 2. The model was able to successfully
346 predict the %HIA for six compounds in the test set within a minimum of 0.29 % and a
347 maximum of 10.97 % difference between the predicted %HIA and the published %HIA. The
348 model underestimated the %HIA for piroxicam where its predicted value for human intestinal
349 absorption was found to be 82.65 % against a literature value of 99 % experimentally
350 obtained in humans. However, the obtained predicted value was found to be closer to a
351 literature value of 89 % for piroxicam's intestinal absorption in dogs⁷¹. An overall close
352 agreement was shown between literature and predicted values of %HIA in Figure 8.

353

354 Prediction of HIA using static cells:

355
$$\text{logit HIA} = 0.515 - 0.4294 \text{ nHD} - 0.006005 V_M - 0.453 \log K_p$$

356 The model's $R^2 = 86.61\%$, $R^2_{\text{adjust.}} = 83.74\%$, $R^2_{\text{PRED}} = 79.67\%$, $S = 0.253$

357 A 95 % confidence interval for $\log K_p$ is given by (-0.874, -0.031). t-statistic and
358 standardised coefficient of $\log K_p$ are -2.3 ($p < 0.05$) and -0.261 respectively suggesting the
359 statistical significance of $\log K_p$ as a predictor. Also the F-ratio of the overall model is
360 statistically significant, $F = 30.19$ and P value 0.000 ($p < 0.05$). A Durbin- Watson statistic
361 value of 2.105 proved the absence of autocorrelation in the current regression model. There
362 was no marked relationship between residuals and predicted values. Seven compounds
363 (carbamazepine, fenoprofen, indomethacin, linezolid, piroxicam, quinine and zolmitriptan)
364 were used for testing the obtained model. As shown in Table 3, the model was able to
365 successfully predict the %HIA for six compounds in the test set within a minimum of 0.6 %
366 and a maximum of 12.60 % difference between the predicted %HIA and the published

367 %HIA. The model underestimated the %HIA for piroxicam where its predicted value for
368 %HIA was found to be 80.73 % against a literature value of 99 % experimentally obtained in
369 humans (see reference in Table 2). However, the obtained predicted value was found to be
370 closer to a literature value of 89 % for piroxicam's intestinal absorption in dogs⁷¹. The
371 model's good predictive power is shown in Figure 9.

372 The final model equation included permeability coefficient, number of hydrogen bond donors
373 and molar volume which all correlate well with the absorption values in the human intestine.
374 Since the permeability coefficient is independent of the donor concentration⁸² and it
375 describes an intrinsic property of the solute to permeate across a specific medium (e.g.
376 intestine) which is independent of the dose but influenced by the applied vehicle⁸³.
377 Therefore, this intrinsic property could be related to one or more of the previously reported
378 physicochemical properties of the permeating solutes in this study. According to literature,
379 molar volume (V_M) encodes for hydrophobic and dispersion forces while hydrogen bond
380 acceptor basicity (nHA) accounts for orientation and induction forces⁸⁴. Both of these
381 parameters are considered as factors of solute lipophilicity as it can be factorised in to two
382 sets which are hydrophobicity which accounts for hydrophobic and dispersion forces and also
383 polar terms which account for hydrogen bonds, orientation and induction forces⁸⁴. The
384 mechanisms of drug-biomembrane interactions involve partitioning in to the hydrophobic
385 core of the membrane which consequently involves the lipophilicity term. Therefore, the
386 descriptors involved in the final model equation show an important impact in the permeation
387 process and also confirm the success of such a technique in the simulation of intestinal
388 membrane for prediction of HIA. However, it should be noted that the majority of the
389 compounds analysed in this work displayed a comparatively high percentage absorption (as is
390 often the case for pharmaceutical compounds) and therefore the predictive ability for
391 compounds with a low absorption should be carefully considered.

392

393 **4. Conclusion**

394 Drug-loaded sodium deoxycholate (NaDC) hydrogels were utilised as the donor phase to
395 study release-permeability using flow-through and static diffusion cells. Furthermore,
396 determination of K_p from the permeation of a number of compounds from the prepared NaDC
397 hydrogels using flow-through cells and static cells was successful in the development of
398 models of high predictive capabilities for human intestinal absorption by using the
399 experimentally obtained K_p . Overall, the two permeation methods yielded highly predictive
400 models of %HIA. Although static cells presented a cheaper option, flow through cells could

401 be considered as a better method as it requires smaller volumes of buffer solution and tested
402 samples in addition to the easier sample collection. NaDC, being a natural physiological
403 surfactant and having gelation properties in the presence of certain factors, has facilitated the
404 creation of a simulation of a biological membrane to mimic the absorption process inside the
405 human intestine which makes it a good alternative for the use of animals in the prediction of
406 human intestinal absorption of pharmaceutical compounds. At present, the proposed system
407 may require more drug than ideally desired within early stage development in industry to
408 complete the analysis yet it does present clear advantages as a novel analytical system. For
409 example, this technique has the advantage of being a much cheaper alternative to the classical
410 *in vitro* cell culture based models (e.g. Caco-2 cells) and membrane based models (e.g.
411 PAMPA) also it is less time consuming and laboratory intensive.

412

413 **References:**

- 414 1. Prentis, R., Y. Lis, and S. Walker, *Pharmaceutical innovation by the seven UK-owned*
415 *pharmaceutical companies (1964-1985)*. British journal of clinical pharmacology, 1988. **25**(3):
416 p. 387-396.
- 417 2. Kennedy, T., *Managing the drug discovery/development interface*. Drug discovery today,
418 1997. **2**(10): p. 436-444.
- 419 3. Venkatesh, S. and R.A. Lipper, *Role of the development scientist in compound lead selection*
420 *and optimization*. Journal of pharmaceutical sciences, 2000. **89**(2): p. 145-154.
- 421 4. Arlington, S., *Pharma 2005-An industrial revolution in R&D*. Pharmaceutical Executive, 2000.
422 **20**(1): p. 74-85.
- 423 5. Qiao, Y., et al., *Unique temperature-dependent supramolecular self-assembly: from*
424 *hierarchical 1D nanostructures to super hydrogel*. The Journal of Physical Chemistry B, 2010.
425 **114**(36): p. 11725-11730.
- 426 6. Dastidar, P., *Supramolecular gelling agents: can they be designed?* Chemical Society
427 Reviews, 2008. **37**(12): p. 2699-2715.
- 428 7. van Esch, J.H., *We can design molecular gelators, but do we understand them?* Langmuir,
429 2009. **25**(15): p. 8392-8394.
- 430 8. Song, F., et al., *Viscoelastic and fractal characteristics of a supramolecular hydrogel*
431 *hybridized with clay nanoparticles*. Colloids and Surfaces B: Biointerfaces, 2010. **81**(2): p.
432 486-491.
- 433 9. Löfman, M., et al., *Bile acid alkylamide derivatives as low molecular weight organogelators:*
434 *Systematic gelation studies and qualitative structural analysis of the systems*. Journal of
435 colloid and interface science, 2011. **360**(2): p. 633-644.
- 436 10. Rub, M.A. and A.Z. Naqvi, *Aqueous amphiphilic drug (amitriptyline hydrochloride)-bile salt*
437 *mixtures at different temperatures*. Colloids and Surfaces B: Biointerfaces, 2011. **84**(2): p.
438 285-291.
- 439 11. Song, S., et al., *Temperature regulated supramolecular structures via modifying the balance*
440 *of multiple non-covalent interactions*. Soft Matter, 2013. **9**(16): p. 4209-4218.
- 441 12. Sievänen, E., *Exploitation of bile acid transport systems in prodrug design*. Molecules, 2007.
442 **12**(8): p. 1859-1889.
- 443 13. Mukhopadhyay, S. and U. Maitra, *Chemistry and biology of bile acids*. Current Science, 2004.
444 **87**(12): p. 1666-1683.

- 445 14. Kiyonaka, S., et al., *Semi-wet peptide/protein array using supramolecular hydrogel*. Nature
446 materials, 2004. **3**(1): p. 58.
- 447 15. Chen, L., et al., *Effect of molecular structure on the properties of naphthalene– dipeptide*
448 *hydrogelators*. Langmuir, 2010. **26**(16): p. 13466-13471.
- 449 16. Lin, Y., et al., *Self-assembled laminated nanoribbon-directed synthesis of noble metallic*
450 *nanoparticle-decorated silica nanotubes and their catalytic applications*. Journal of Materials
451 Chemistry, 2012. **22**(35): p. 18314-18320.
- 452 17. Travaglini, L., et al., *Twisted nanoribbons from a RGD-bearing cholic acid derivative*. Colloids
453 and Surfaces B: Biointerfaces, 2017. **159**: p. 183-190.
- 454 18. Tsigotis-Maniecka, M., R. Gancarz, and K.A. Wilk, *Polysaccharide hydrogel particles for*
455 *enhanced delivery of hesperidin: Fabrication, characterization and in vitro evaluation*.
456 Colloids and Surfaces A: Physicochemical and Engineering Aspects, 2017. **532**: p. 48-56.
- 457 19. Cheng, X., et al., *An injectable, dual pH and oxidation-responsive supramolecular hydrogel for*
458 *controlled dual drug delivery*. Colloids and Surfaces B: Biointerfaces, 2016. **141**: p. 44-52.
- 459 20. Sun, X., et al., *Manipulation of the gel behavior of biological surfactant sodium deoxycholate*
460 *by amino acids*. The Journal of Physical Chemistry B, 2014. **118**(3): p. 824-832.
- 461 21. Calabresi, M., P. Andreatti, and C. La Mesa, *Supra-molecular association and polymorphic*
462 *behaviour in systems containing bile acid salts*. Molecules, 2007. **12**(8): p. 1731-1754.
- 463 22. Wang, D. and J. Hao, *Self-assembly fibrillar network gels of simple surfactants in organic*
464 *solvents*. Langmuir, 2011. **27**(5): p. 1713-1717.
- 465 23. Yuan, Z., et al., *Gel phase originating from molecular quasi-crystallization and nanofiber*
466 *growth of sodium laurate–water system*. Soft Matter, 2008. **4**(8): p. 1639-1644.
- 467 24. CAO, X.-L., et al., *Interactions between anionic surfactants and cations*. Acta Physico-Chimica
468 Sinica, 2010. **26**(7): p. 1959-1964.
- 469 25. Jover, A., et al., *Dynamic rheology of sodium deoxycholate gels*. Langmuir, 2002. **18**(4): p.
470 987-991.
- 471 26. Murata, Y., et al., *Study of the micelle formation of sodium deoxycholate. Concentration*
472 *dependence of carbon-13 nuclear magnetic resonance chemical shift*. The Journal of Physical
473 Chemistry, 1982. **86**(24): p. 4690-4694.
- 474 27. Rothen-Rutishauser, B., et al., *A newly developed in vitro model of the human epithelial*
475 *airway barrier to study the toxic potential of nanoparticles*. Altex, 2008. **25**(3): p. 191-196.
- 476 28. Paixão, P., L.F. Gouveia, and J.A. Morais, *Prediction of the in vitro permeability determined in*
477 *Caco-2 cells by using artificial neural networks*. European Journal of Pharmaceutical Sciences,
478 2010. **41**(1): p. 107-117.
- 479 29. Thomas, S., et al., *Simulation modelling of human intestinal absorption using Caco-2*
480 *permeability and kinetic solubility data for early drug discovery*. Journal of pharmaceutical
481 sciences, 2008. **97**(10): p. 4557-4574.
- 482 30. Camenisch, G., G. Folkers, and H. van de Waterbeemd, *Comparison of passive drug transport*
483 *through Caco-2 cells and artificial membranes*. International journal of pharmaceuticals, 1997.
484 **147**(1): p. 61-70.
- 485 31. Subramanian, G. and D.B. Kitchen, *Computational approaches for modeling human intestinal*
486 *absorption and permeability*. Journal of molecular modeling, 2006. **12**(5): p. 577-589.
- 487 32. Hou, T., et al., *ADME evaluation in drug discovery. 5. Correlation of Caco-2 permeation with*
488 *simple molecular properties*. Journal of chemical information and computer sciences, 2004.
489 **44**(5): p. 1585-1600.
- 490 33. Reynolds, D.P., et al., *Ionization-specific analysis of human intestinal absorption*. Journal of
491 pharmaceutical sciences, 2009. **98**(11): p. 4039-4054.
- 492 34. Bock, U., T. Flötotto, and E. Haltner, *Validation of cell culture models for the intestine and the*
493 *blood brain barrier and comparison of drug permeation*. Altex, 2004. **21**(Suppl 3): p. 57-64.
- 494 35. Augustijns, P. and R. Mols, *HPLC with programmed wavelength fluorescence detection for*
495 *the simultaneous determination of marker compounds of integrity and P-gp functionality in*

- 496 *the Caco-2 intestinal absorption model*. Journal of pharmaceutical and biomedical analysis,
497 2004. **34**(5): p. 971-978.
- 498 36. Bujard, A., et al., *Predicting both passive intestinal absorption and the dissociation constant*
499 *toward albumin using the PAMPA technique*. European Journal of Pharmaceutical Sciences,
500 2014. **63**: p. 36-44.
- 501 37. Zhu, C., et al., *A comparative study of artificial membrane permeability assay for high*
502 *throughput profiling of drug absorption potential*. European journal of medicinal chemistry,
503 2002. **37**(5): p. 399-407.
- 504 38. Akamatsu, M., et al., *In silico prediction of human oral absorption based on QSAR analyses of*
505 *PAMPA permeability*. Chemistry & biodiversity, 2009. **6**(11): p. 1845-1866.
- 506 39. Nielsen, P.E. and A. Avdeef, *PAMPA—a drug absorption in vitro model: 8. Apparent filter*
507 *porosity and the unstirred water layer*. European journal of pharmaceutical sciences, 2004.
508 **22**(1): p. 33-41.
- 509 40. Rogers, S.M., D. Back, and M. Orme, *Intestinal metabolism of ethinyloestradiol and*
510 *paracetamol in vitro: studies using Ussing chambers*. British journal of clinical pharmacology,
511 1987. **23**(6): p. 727-734.
- 512 41. Smith, P., et al., *Intestinal 5-fluorouracil absorption: Use of Ussing chambers to assess*
513 *transport and metabolism*. Pharmaceutical research, 1988. **5**(9): p. 598-603.
- 514 42. Annaert, P., et al., *In vitro, ex vivo, and in situ intestinal absorption characteristics of the*
515 *antiviral ester prodrug adefovir dipivoxil*. Journal of pharmaceutical sciences, 2000. **89**(8): p.
516 1054-1062.
- 517 43. Kim, J.-S., et al., *The suitability of an in situ perfusion model for permeability determinations:*
518 *utility for BCS class I biowaiver requests*. Molecular pharmaceutics, 2006. **3**(6): p. 686-694.
- 519 44. Zakeri-Milani, P., et al., *Predicting human intestinal permeability using single-pass intestinal*
520 *perfusion in rat*. J Pharm Pharm Sci, 2007. **10**(3): p. 368-379.
- 521 45. Sun, L., et al., *Structure-based prediction of human intestinal membrane permeability for*
522 *rapid in silico BCS classification*. Biopharmaceutics & drug disposition, 2013. **34**(6): p. 321-
523 335.
- 524 46. Doluisio, J.T., et al., *Drug absorption I: An in situ rat gut technique yielding realistic*
525 *absorption rates*. Journal of pharmaceutical sciences, 1969. **58**(10): p. 1196-1200.
- 526 47. Neirinckx, E., *Towards a veterinary biopharmaceutics classification system: oral*
527 *bioavailability and ex vivo intestinal permeability studies of paracetamol and ketoprofen in*
528 *different animal species*. 2010, Ghent University.
- 529 48. Waters, L.J., et al., *The use of bile salt micelles for the prediction of human intestinal*
530 *absorption*. Journal of pharmaceutical sciences, 2016. **105**(12): p. 3611-3614.
- 531 49. Waters, L.J., D.S. Shokry, and G. Parkes, *Predicting human intestinal absorption in the*
532 *presence of bile salt with micellar liquid chromatography*. Biomedical Chromatography,
533 2016. **30**(10): p. 1618-1624.
- 534 50. Franz, T.J., *Percutaneous absorption. On the relevance of in vitro data*. Journal of
535 Investigative Dermatology, 1975. **64**(3): p. 190-195.
- 536 51. Bartosova, L. and J. Bajgar, *Transdermal drug delivery in vitro using diffusion cells*. Current
537 medicinal chemistry, 2012. **19**(27): p. 4671-4677.
- 538 52. PermeGear, *Diffusion Testing Fundamentals*. 2015.
- 539 53. <http://www.chemspider.com/>, December, 2014.
- 540 54. <http://www.drugbank.ca/>, December, 2014.
- 541 55. Norinder, U., T. Österberg, and P. Artursson, *Theoretical calculation and prediction of*
542 *intestinal absorption of drugs in humans using MolSurf parametrization and PLS statistics*.
543 European journal of pharmaceutical sciences, 1999. **8**(1): p. 49-56.
- 544 56. Raevsky, O.A., et al., *Quantitative Estimation of Drug Absorption in Humans for Passively*
545 *Transported Compounds on the Basis of Their Physico-chemical Parameters*. Quantitative
546 Structure-Activity Relationships, 2000. **19**(4): p. 366-374.

- 547 57. Zhao, Y.H., et al., *Rate-limited steps of human oral absorption and QSAR studies*.
548 Pharmaceutical research, 2002. **19**(10): p. 1446-1457.
- 549 58. Rhodes, H., et al., *Differentiating nonaqueous titration of aspirin, acetaminophen, and*
550 *salicylamide mixtures*. Journal of pharmaceutical sciences, 1975. **64**(8): p. 1386-1388.
- 551 59. Martin, A., *Physical pharmacy: Physical chemical principles in the pharmaceutical sciences*.
552 2nd ed. ed. 1969, Philadelphia: Lea & Febiger.
- 553 60. Shayanfar, A., S. Velaga, and A. Jouyban, *Solubility of carbamazepine, nicotinamide and*
554 *carbamazepine–nicotinamide cocrystal in ethanol–water mixtures*. Fluid Phase Equilibria,
555 2014. **363**: p. 97-105.
- 556 61. <http://www.pharminfotech.co.nz/manual/Formulation/mixtures/fluconazole.html>, April,
557 2015.
- 558 62. <https://pubchem.ncbi.nlm.nih.gov/>, December, 2014.
- 559 63. http://www.chemicalbook.com/ProductMSDSDetailCB9154247_EN.htm, April, 2015.
- 560 64. Janssen, P.A., et al., *Chemistry and pharmacology of CNS depressants related to 4-(4-*
561 *hydroxy-4-phenylpiperidino) butyrophenone. Part I: Synthesis and screening data in mice*. J.
562 med. pharm. Chem, 1959. **1**: p. 281-297.
- 563 65. information, U.p., 1975.
- 564 66. NARAHASHI, T., D.T. FRAZIER, and M. YAMADA, *The site of action and active form of local*
565 *anesthetics. I. Theory and pH experiments with tertiary compounds*. Journal of Pharmacology
566 and Experimental Therapeutics, 1970. **171**(1): p. 32-44.
- 567 67. <https://comptox.epa.gov/dashboard/dsstoxdb/results?search=DTXSID1045166#toxval>, April,
568 2015.
- 569 68. Stella, V. and J. Pipkin, *Phenylbutazone ionization kinetics*. Journal of pharmaceutical
570 sciences, 1976. **65**(8): p. 1161-1165.
- 571 69. Ballard, B.E. and E. Nelson, *Physicochemical properties of drugs that control absorption rate*
572 *after subcutaneous implantation*. Journal of Pharmacology and Experimental Therapeutics,
573 1962. **135**(1): p. 120-127.
- 574 70. Patel, S.R., et al., *Controlled non-invasive transdermal iontophoretic delivery of zolmitriptan*
575 *hydrochloride in vitro and in vivo*. European Journal of Pharmaceutics and Biopharmaceutics,
576 2009. **72**(2): p. 304-309.
- 577 71. Musther, H., et al., *Animal versus human oral drug bioavailability: Do they correlate?*
578 European Journal of Pharmaceutical Sciences, 2014. **57**: p. 280-291.
- 579 72. Castillo-Garit, J., et al., *Prediction of ADME properties, Part 1: Classification models to predict*
580 *Caco-2 cell permeability using atom-based bilinear indices*. Afinidad, 2014. **71**(566).
- 581 73. Yan, A., Z. Wang, and Z. Cai, *Prediction of human intestinal absorption by GA feature*
582 *selection and support vector machine regression*. International journal of molecular sciences,
583 2008. **9**(10): p. 1961-1976.
- 584 74. Varma, M.V., K. Sateesh, and R. Panchagnula, *Functional role of P-glycoprotein in limiting*
585 *intestinal absorption of drugs: contribution of passive permeability to P-glycoprotein*
586 *mediated efflux transport*. Molecular pharmaceutics, 2005. **2**(1): p. 12-21.
- 587 75. Paixão, P., L.F. Gouveia, and J.A. Morais, *Prediction of the human oral bioavailability by using*
588 *in vitro and in silico drug related parameters in a physiologically based absorption model*.
589 International journal of pharmaceutics, 2012. **429**(1): p. 84-98.
- 590 76. Hou, T., et al., *ADME evaluation in drug discovery. 7. Prediction of oral absorption by*
591 *correlation and classification*. Journal of chemical information and modeling, 2007. **47**(1): p.
592 208-218.
- 593 77. Molero-Monfort, M., et al., *Biopartitioning micellar chromatography: an in vitro technique*
594 *for predicting human drug absorption*. Journal of Chromatography B: Biomedical Sciences
595 and Applications, 2001. **753**(2): p. 225-236.

- 596 78. Newby, D., A.A. Freitas, and T. Ghafourian, *Decision trees to characterise the roles of*
 597 *permeability and solubility on the prediction of oral absorption*. European journal of
 598 *medicinal chemistry*, 2015. **90**: p. 751-765.
- 599 79. Veber, D.F., et al., *Molecular properties that influence the oral bioavailability of drug*
 600 *candidates*. Journal of medicinal chemistry, 2002. **45**(12): p. 2615-2623.
- 601 80. Chu, K.A., *Predicting Passive Intestinal Drug Absorption: An Interesting Relationship between*
 602 *Fraction Absorbed and Melting Point*. 2009.
- 603 81. Kansy, M., F. Senner, and K. Gubernator, *Physicochemical high throughput screening:*
 604 *parallel artificial membrane permeation assay in the description of passive absorption*
 605 *processes*. Journal of medicinal chemistry, 1998. **41**(7): p. 1007-1010.
- 606 82. Koláčková, L., *Comparative in vitro study of permeation of selected drugs from lipophilic*
 607 *solutions through human skin*. 2007: p. 10.
- 608 83. Dragicevic, N. and H.I. Maibach, *Percutaneous Penetration Enhancers Drug Penetration*
 609 *Into/through the Skin: Methodology and General Considerations*. 2017: Springer.
- 610 84. Liu, X., B. Testa, and A. Fahr, *Lipophilicity and its relationship with passive drug permeation*.
 611 *Pharmaceutical research*, 2011. **28**(5): p. 962-977.
- 612 85. Deconinck, E., et al., *Evaluation of chromatographic descriptors for the prediction of gastro-*
 613 *intestinal absorption of drugs*. Journal of Chromatography A, 2007. **1138**(1): p. 190-202.

614

615 **LEGENDS**616 **Table 1.** A summary of molecular descriptors for the selected twenty-five drugs.

617 **Table 2:** Permeability coefficient ($\log K_p$) experimentally obtained from flow-through cells,
 618 predicted %HIA (Pred. %HIA) and experimentally determined literature %HIA (Expt. %
 619 HIA) values for the compounds analysed including seven validation compounds (*).

620

621 **Table 3:** Permeability coefficient ($\log K_p$) experimentally obtained from static cells,
 622 predicted %HIA (Pred. %HIA) and experimentally determined literature %HIA (Expt.
 623 %HIA) values for the compounds analysed including seven validation compounds (*).

624

625 **Fig. 1.** Schematic representation of the formed salt-induced NaDC gels²⁰.

626

627 **Fig. 2.** A diagrammatic representation of a static cell (left) and flow through cell
 628 (right) (reference⁵²).

629

630 **Fig. 3.** SEM images of gel formed by 70 mM NaDC of magnification power x1000 (left) and
 631 x1300 (right).

632 **Fig. 4.** SEM images for a) carbamazepine 70 mM hydrogel and b) meloxicam 70 mM
 633 hydrogel

634

635 **Fig. 5.** Permeability coefficients (K_p) of eight selected drugs at three different concentrations
 636 of NaDC hydrogels.

637 **Fig. 6.** Plot of cumulative permeated amount of eight selected drugs against time obtained
638 using flow-through cells.

639

640 **Fig. 7.** Plot of cumulative permeated amount of eight selected drugs against time obtained
641 using static cells.

642

643 **Fig. 8.** Regression plot of predicted %HIA values against literature %HIA.

644

645 **Fig. 9.** Regression plot of predicted %HIA values against literature %HIA.

646

647

648

649

650

651

Table 1

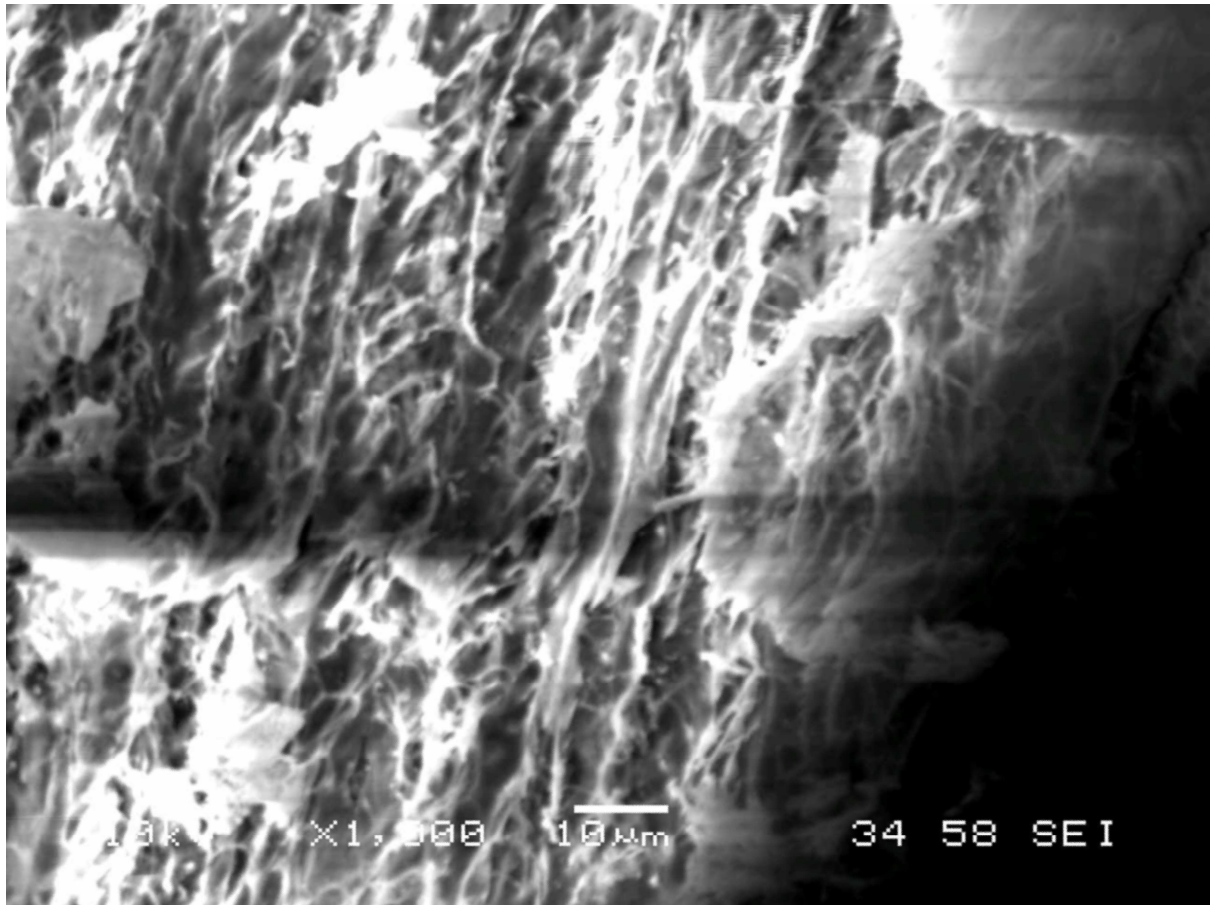
Drug	Mwt ⁵³	pK_a ⁵⁴	S_w ⁵⁴	HD ⁵³	HA ⁵³	RB ⁵³	V_M ⁵³
Acetaminophen	151.20	9.9 ⁵⁸	14	2	3	1	131.1
Caffeine	194.20	14 ⁵⁹	21.6	0	6	0	133.4
Carbamazepine	236.36	13.9	0.21 ^{54, 54, 60}	2, 1 ⁵⁴	3	0	186.6
Cimetidine	252.34	6.8	9.38	3	6	8	198.2
Diclofenac	296.20	4.15	0.00237	2	3	4	206.8
Fenoprofen	242.27	4.5	0.033 ⁵³	1	3	4	204.7
Fluconazole	306.27	12.71	9 ⁶¹	1	7	5	205.3
Flurbiprofen	244.26	4.42	0.008	1	2	3	203.6
Fosinopril	563.66	-4.4	0.00101	1	8	15	480.4
Gemfibrozil	250.33	4.5 ⁶²	0.13 ⁶³	1	3	6	239.7
Haloperidol	375.86	8.3 ⁶⁴	0.014	1	3	6	303.3
Ibuprofen	206.30	5.2 ⁶⁵	0.0684	1	2	4	200.3
Indomethacin	357.79	4.5	0.000937	1	5	4	269.6
Ketoprofen	254.30	3.88	0.051	1	3	4	212.2
Leflunomide	270.21	-0.45	0.021	1	4	3	194.1
Lidocaine	234.40	7.9 ⁶⁶	0.2337 ⁶⁷	1	3	5	238.8
Linezolid	337.35	-0.66	1.44	1	7	4	259.0
Meloxicam	351.40	4.08	0.00715	2	7	2	220.3
Moexipril	498.57	5.2	0.00585	2	9	12	408.1
Naproxen	230.26	4.15	0.0159	1	3	3	192.3
Phenylbutazone	308.37	4.4 ⁶⁸	0.7 ⁶²	0	4	5	262.8
Piroxicam	331.35	6.3	0.023	2	7	2	222.8
Quinine	324.42	4.2	0.5	1	4	4	266.4
Theophylline	180.16	8.8 ⁶⁹	22.9	1	6	0	122.9
Zolmitriptan	287.36	9.52 ⁷⁰	0.19	2	5	5	236.1

Table 2

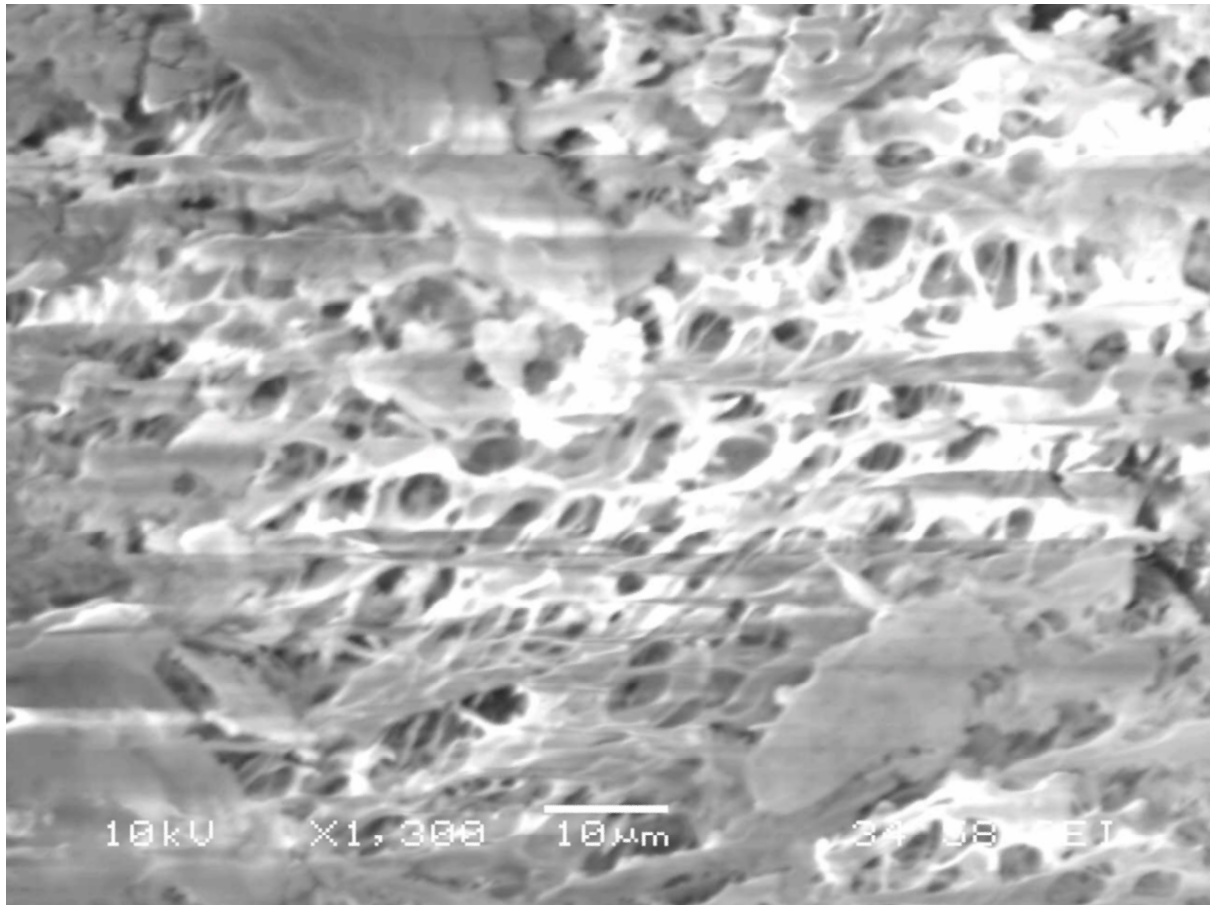
Drug	Expt. %HIA	Pred. %HIA	Expt. %HIA- Pred. %HIA
Acetaminophen	80 ⁷²	84.32	-4.32
Caffeine	99 ⁷³	98.87	0.13
Carbamazepine*	70 ⁷⁴	69.71	0.29
Cimetidine	60 ⁷²	57.13	2.87
Diclofenac	81 ^{75, 76}	88.02	-7.02
Fenoprofen*	85 ⁷⁶	95.97	-10.97
Fluconazole	94 ⁷³	92.76	1.24
Flurbiprofen	95 ⁷⁷	93.69	1.31
Fosinopril	35 ⁷⁸	35.68	-0.68
Gemfibrozil	95 ⁷⁵	92.66	2.34
Haloperidol	60 ⁷⁹	49.70	10.3
Ibuprofen	85 ⁷⁵	94.07	-9.07
Indomethacin	98 ⁷⁹	95.38	2.62
Ketoprofen	96 ⁷²	93.67	2.33
Leflunomide	80 ⁷⁸	89.14	-9.14
Lidocaine	90 ⁷⁷	88.14	1.86
Linezolid*	100 ⁷⁸	91.16	8.84
Meloxicam	90 ⁷²	76.70	13.3
Moexipril	23 ⁷⁸	37.83	-14.83
Naproxen*	94 ⁷²	95.06	-1.06
Phenylbutazone	96 ^{73, 79, 80}	97.45	-1.45
Piroxicam*	99 ⁸⁰	82.65	16.35
Quinine*	95 ⁷⁷	96.72	-1.72
Theophylline	98 ⁸¹	98.41	-0.41
Zolmitriptan*	70 ^{71, 78}	68.01	1.99

Table 3

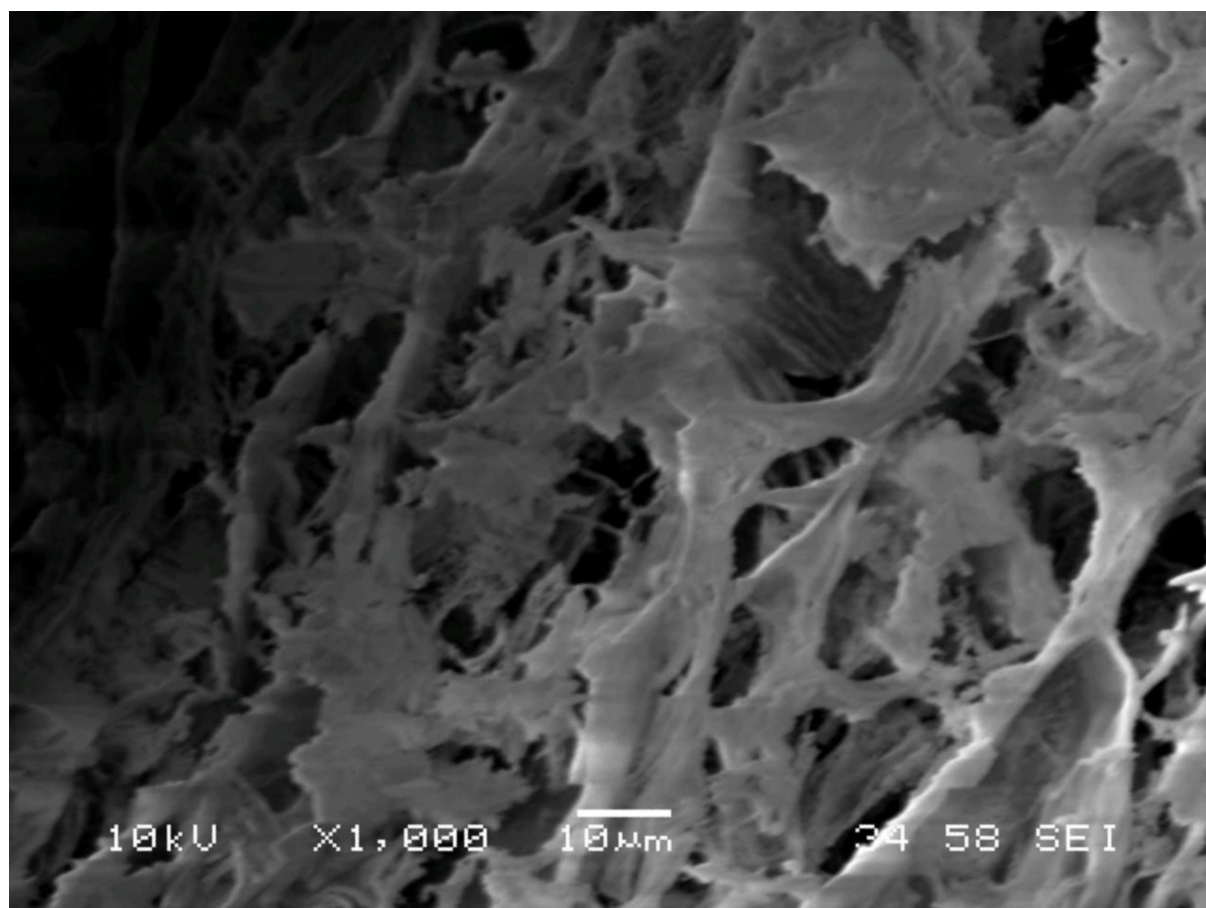
Drug	Expt. %HIA	Pred. %HIA
Acetaminophen	80 ⁷²	88.97
Caffeine	99 ⁷³	98.24
Carbamazepine*	70 ⁷⁴	70.60
Cimetidine	60 ⁷²	57.16
Diclofenac	81 ^{75, 76}	85.47
Fenoprofen*	85 ⁷⁶	92.37
Fluconazole	94 ⁷³	93.77
Flurbiprofen	95 ⁷⁷	91.79
Fosinopril	35 ⁷⁸	34.68
Gemfibrozil	95 ⁷⁵	90.64
Haloperidol	60 ⁷⁹	62.80
Ibuprofen	90 ^{75, 85}	92.01
Indomethacin*	98 ⁷⁹	86.36
Ketoprofen	90 ⁷⁷	89.69
Leflunomide	80 ⁷⁸	86.12
Lidocaine	81 ^{73, 74, 77, 80}	86.71
Linezolid*	100 ⁷⁸	87.40
Meloxicam	90 ⁷²	77.64
Moexipril	23 ⁷⁸	26.55
Naproxen	97 ^{72, 77}	91.95
Phenylbutazone	90 ⁷⁹	94.44
Piroxicam*	99 ⁸⁰	80.73
Quinine*	95 ⁷⁷	93.94
Theophylline	96 ⁸⁵	97.95
Zolmitriptan*	70 ^{71, 78}	70.94



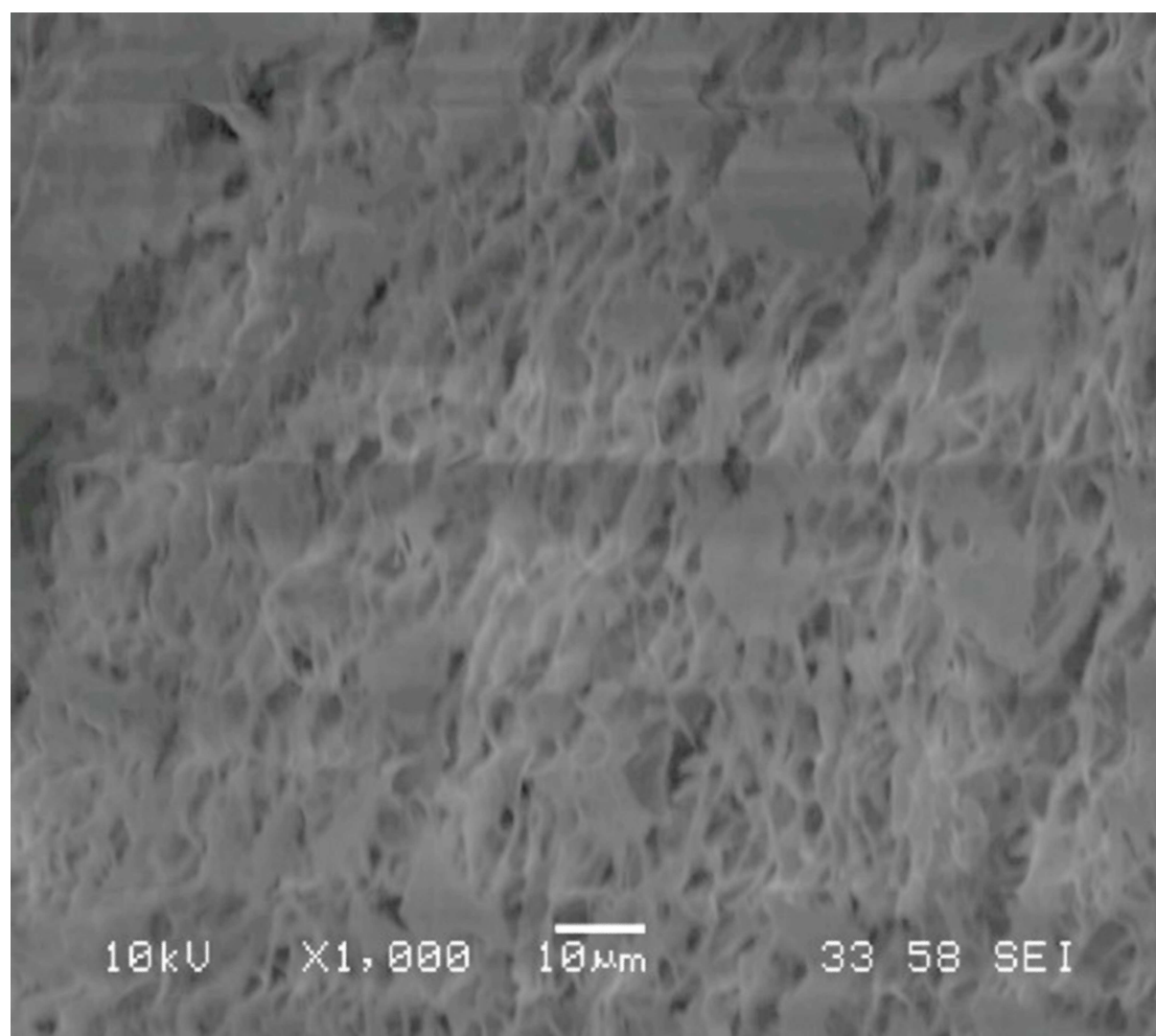
ACCEPTED MANUSCRIPT

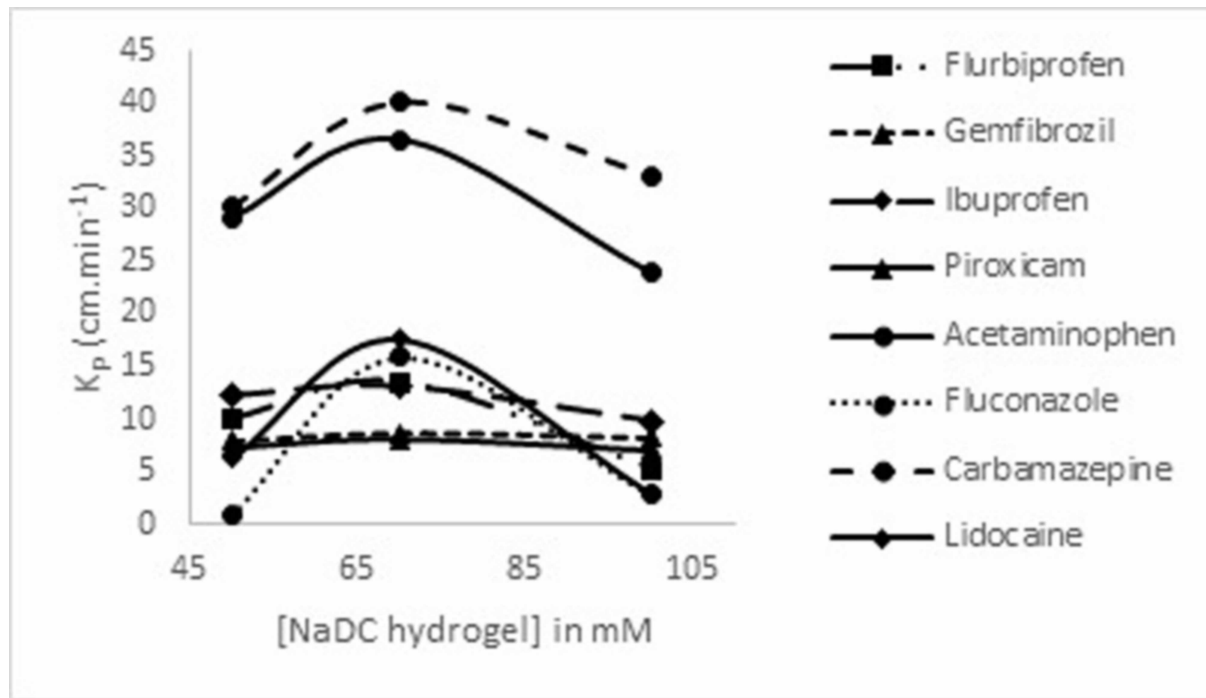


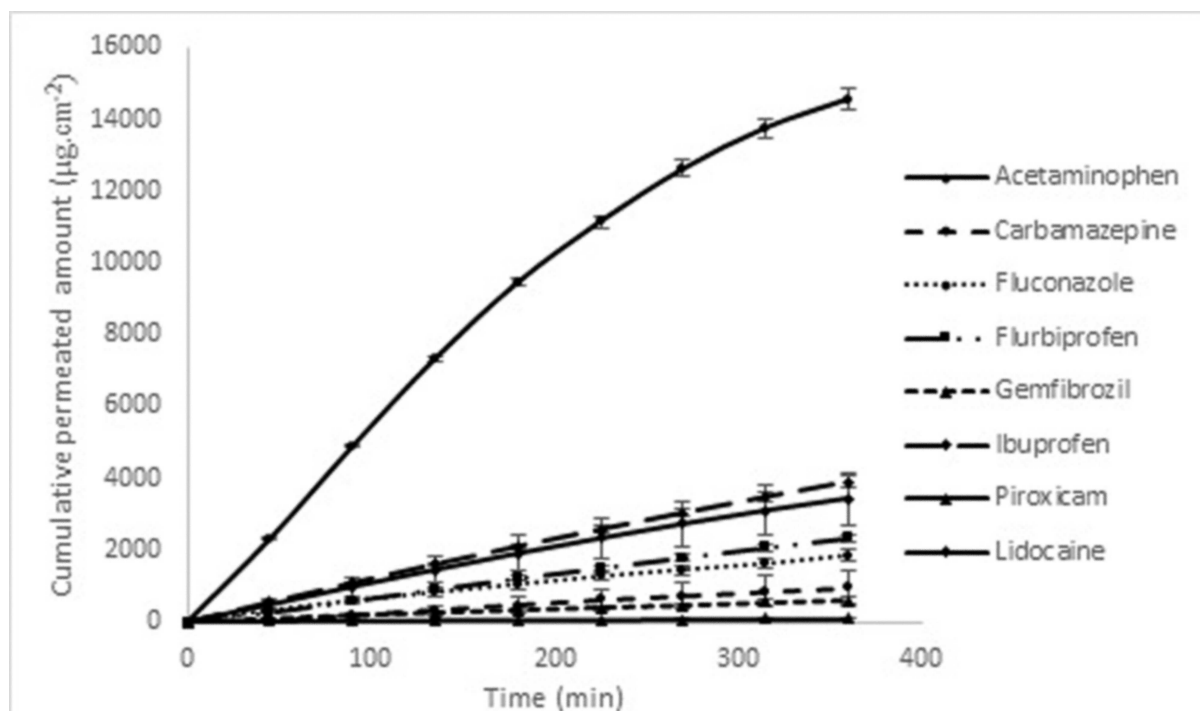
ACCEPTED MANUSCRIPT

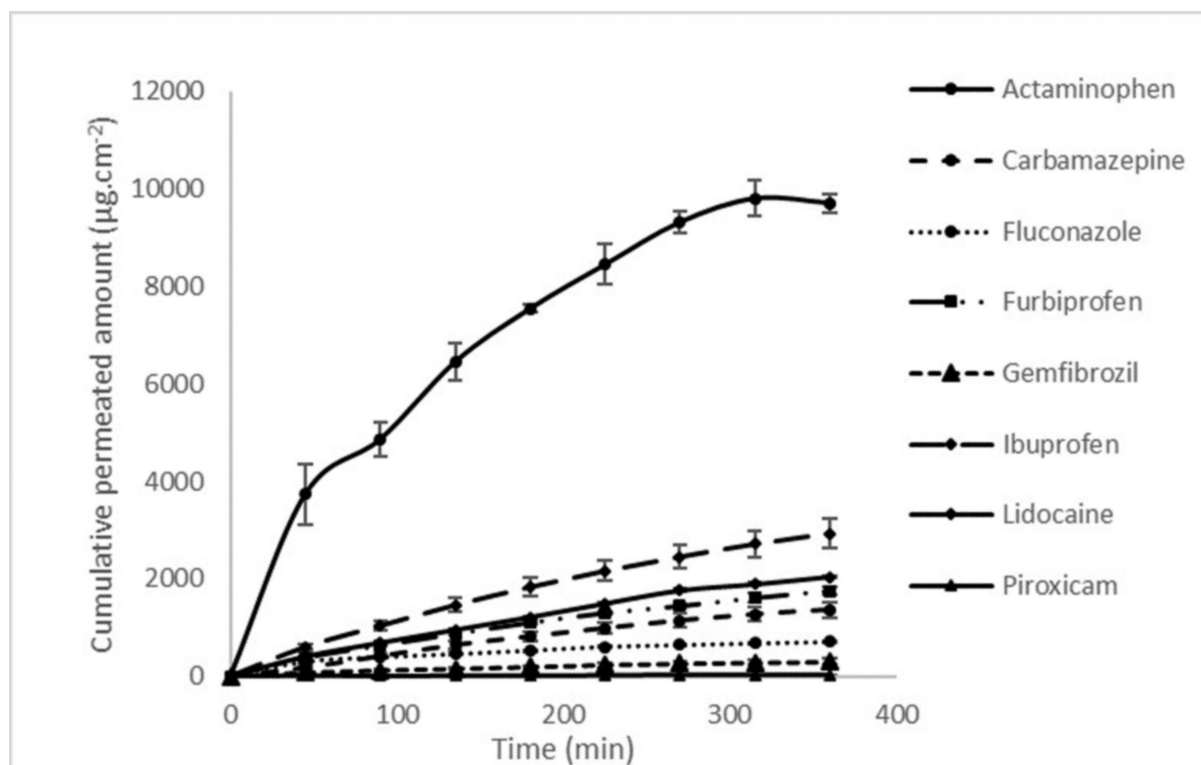


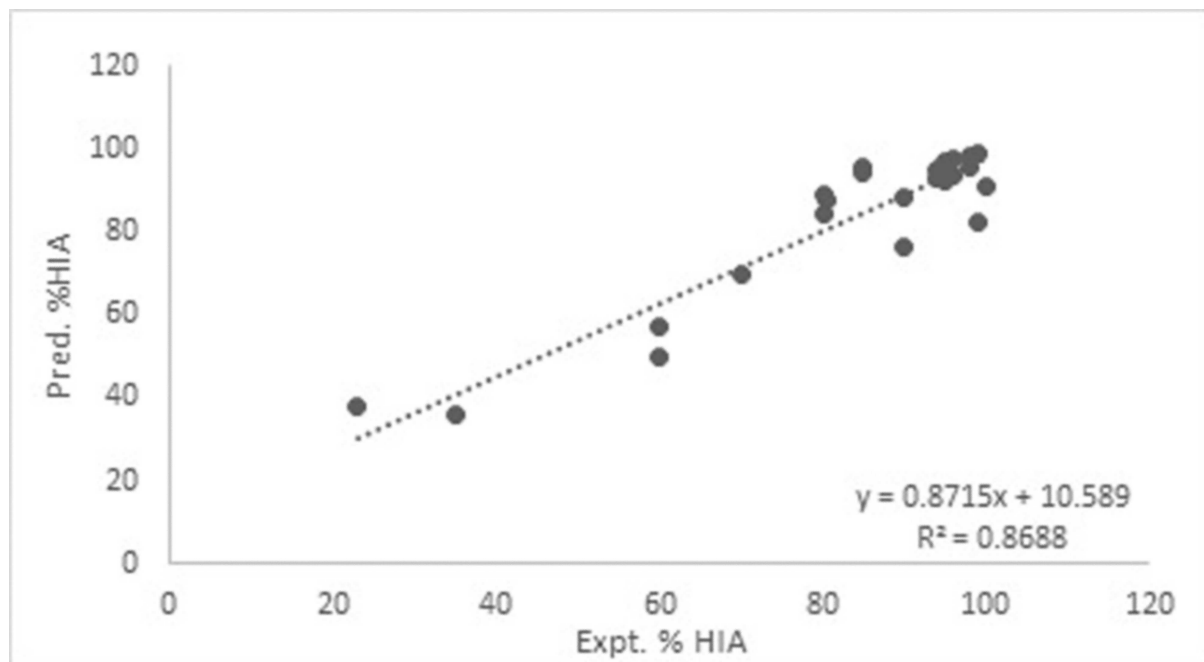
ACCEPTED MANUSCRIPT

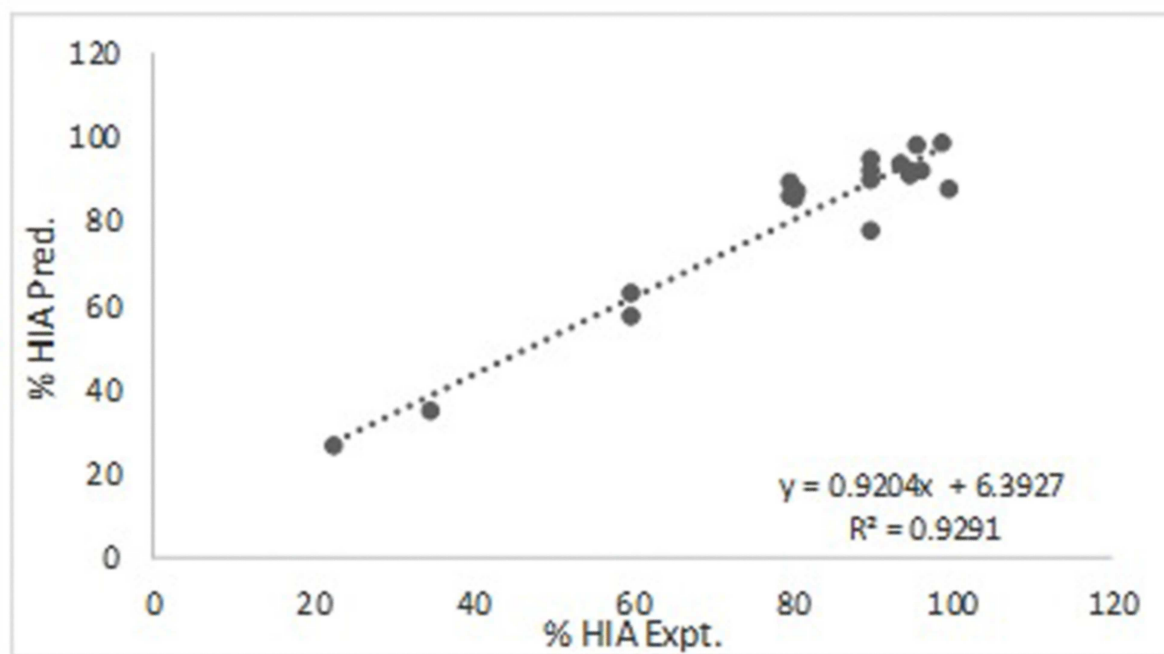




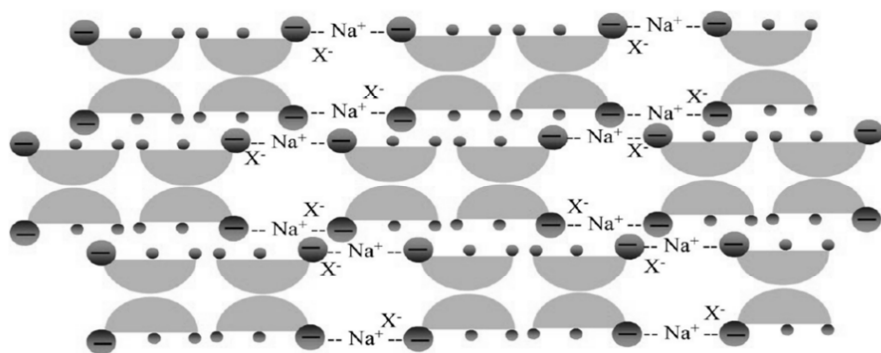




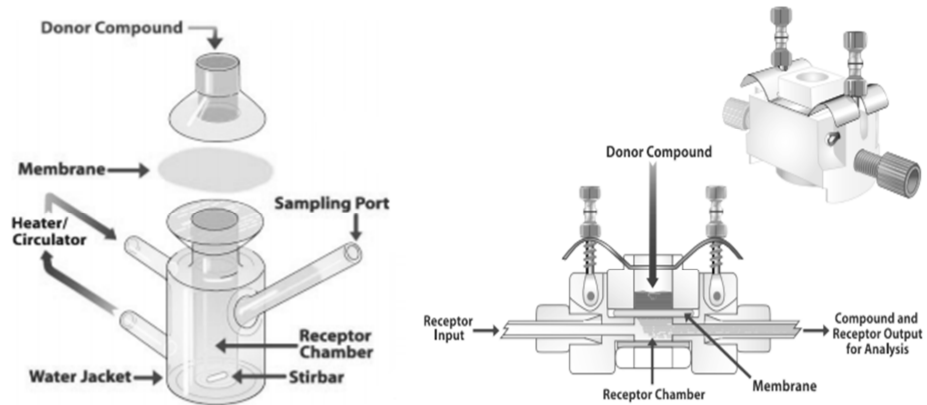




ACCEPTED MANUSCRIPT



ACCEPTED MANUSCRIPT



ACCEPTED MANUSCRIPT